Earth Surface Processes and Landforms
Earth Surf. Process. Landforms **29**, 1235–1258 (2004)
Published online 18 August 2004 in Wiley InterScience (www.interscience.wiley.com). DOI: 10.1002/esp.1088

THE GEOMORPHIC DYNAMICS AND ENVIRONMENTAL HISTORY OF AN UPPER DELTAIC FLOODPLAIN TRACT IN THE SACRAMENTO–SAN JOAQUIN DELTA, CALIFORNIA, USA

K. J. BROWN[1,2]* AND G. B. PASTERNACK[2]

[1] *Department of Biology, Duke University, Durham, North Carolina, USA*
[2] *Department of Land, Air and Water Resources, University of California, Davis, California, USA*

Received 3 January 2003; Revised 15 September 2003; Accepted 12 January 2004

ABSTRACT

A multi-proxy approach was used to examine the geomorphic dynamics and environmental history of an upper deltaic floodplain tract in the Sacramento–San Joaquin Delta, California. Three long cores were collected from the McCormack–Williamson Tract (MWT) and these cores were analyzed for bulk density, loss-on-ignition, fine (clay and silt) content, Al concentration, magnetic susceptibility, pollen, and charcoal. Radiocarbon dates obtained for the cores were converted into calendar years and an age–depth model was constructed. Long-term vertical accretion and sedimentation rates were estimated from the age–depth model. Cross-core relations show that coarse sediment generally accumulates more rapidly and has greater magnetic susceptibility compared to fine sediment. Percentage fine and LOI data show a strong linear relationship that indicates flooding is the primary mechanism for the deposition of particular organic matter on the floodplain and that landscape wash load has contributed a highly consistent fraction of persistent organic matter averaging 5·5 per cent to the site. Down-core grain size profiles show two hydrological domains in the cores, namely millennial fine–coarse fluctuations superimposed on general up-core fining. Coarse sediment is viewed as channel or near-channel overbank deposits, whereas fine deposits are considered to be distal overbank flood deposits. The coarse–fine fluctuations are indicative of changing depositional settings as channels migrated laterally across MWT, whereas the upward fining trend reflects a combination of self-limiting overbank deposition as floodplain elevation increased and decreasing competence as sea-level rise reduced flood-pulse energy slopes. MWT has been cross-cut and incised numerous times in the past, only to have the channels abandoned and subsequently filled by fine sediment. The channels around MWT attained their modern configuration about 4000 years ago. MWT likely came under tidal influence at about 2500 cal BP. Wetlands have recently developed on MWT, but they are inorganic sediment dominated. Copyright © 2004 John Wiley & Sons, Ltd.

KEY WORDS: floodplain; delta; geomorphic dynamics; channel migration; marine transgression; Holocene; California

INTRODUCTION

In comparison to the broad-scale geomorphology of floodplains and intertidal deltas, the fine-scale processes at the interface between the two have received little focus. The floodplain–delta interface is highly important because the processes operating at the interface can influence the formation of oil and gas traps and deposits (Rainwater, 1975; Noble *et al*., 1991) as well as impact the local environmental geology of lands that are often used for agriculture or urban expansion. The interface is also important because its landscape position can yield an integrated perspective on basin-scale paleoenvironmental conditions (Pasternack *et al*., 2001).

Current understanding of the long-term geomorphic processes that characterize floodplains stem from the geomorphic analyses of stratigraphic successions of cutbanks, excavated trenches, and sediment cores. Classically, the two dominant processes driving floodplain evolution are lateral accretion (Wolman and Leopold, 1957) and overbank deposition (Bridge, 1984; Nanson, 1986; Walling and He, 1998; Tornqvist and Bridge, 2002). The relative roles of each vary substantially as a function of allogenic controls such as climate (Brakenridge, 1980; Blum and Tornqvist, 2000), climate variability (Knox, 1993; Goodbred and Kuehl, 1998), basin characteristics (Benda and Dunne, 1997), and human activities (Knox, 1995). Additional important processes that affect floodplains include channel avulsion (Bridge, 1984; Goodbred and Kuehl, 1998; Tornqvist and Bridge, 2002) and organic

* Correspondence to: K. Brown, Department of Biology, Duke University, Box 90338, Durham, NC 27708, USA. E-mail: kendrik@duke.edu

accretion (Mattraw and Elder, 1984; Cotton *et al*., 1999). These processes and still others result in a large number of floodplain forms, which are well summarized by Brown (1997).

Geomorphic processes acting on deltas have also been described through analyses of sedimentary deposits. The dominant processes controlling deltaic evolution are subaqueous sediment input and sediment redistribution (Galloway, 1975; Coleman, 1976). Constraints on long-term deltaic evolution stem from the interdependent process of sea-level change and accommodation (Jervey, 1988; Blum and Tornqvist, 2000). Delta morphology has also been linked to the grain size distribution of sediment input (Orton and Reading, 1993). More recent studies have shown that delta plain evolution is strongly influenced by vegetative controls (Pasternack and Brush, 2001, 2002) and by the floodplain processes described above (Goodbred and Kuehl, 1998).

Attempts to delineate the downstream extent of floodplains (Alexander and Marriott, 1999) and upstream extent of deltas (Coleman, 1976) suggest no distinctive process or morphology on which to base the delineation. Coleman (1976) terms the 'upper deltaic plain' as the region above significant tidal or marine influence that is dominated by riverine depositional processes. Because this zone may be ~100 km inland from the subtidal zone, the potential for wind and tidally transported coastal sediment to play a role is often negligible, though winds and tides may be important in the redistribution of riverine channel and overbank flood sediments. Goodbred and Kuehl (1998) reported that the upper delta plain of the Brahmaputra–Ganges system included significant areas of inactive floodplain that were isolated by channel avulsion.

In this study, a detailed investigation was performed to characterize the processes occurring at the interface between a floodplain and a delta using sedimentological and paleoenvironmental reconstruction techniques. Specific objectives to achieve this characterization of the interface were to (1) develop an age–depth model for a transitional site; (2) document down-core stratigraphic zonation, rates of vertical accretion and sedimentation as well as changes in grain size; (3) characterize the cross-core relations between grain size, accretion, sedimentation, and magnetic susceptibility; (4) assess the relative proportion of vertical accretion due to watershed influx of sediment versus *in situ* biomass accumulation; and (5) examine the fluvial processes operating at the site as well as the evolution of the tract.

STUDY AREA

The Sacramento–San Joaquin Delta is a 299 000 ha inland tidal delta located east of San Francisco Bay in central California with an ~107 000 km^2 drainage basin (Figure 1). According to the classification of Galloway (1975), the delta is dominated by sediment input, with an annual outflow of ~19 billion m^3 of water and suspended sediment annual inflow and outflow of ~4·7 and ~3·3 million metric tons, respectively (Conomos and Peterson, 1976). The lower delta plain shows some morphological influence of winds and mixed tides. Monthly mean wind speed ranges from 2 to 5 m s^{-1} with peak monthly gusts averaging 15–21 m s^{-1} (Conomos and Peterson, 1976). The primary wind direction is up delta. The summer tidal range at the delta front is ~1·4 m and that in upper delta distributary channels is ~1·0 m. The delta has a rejoining distributary channel pattern (*sensu* Coleman, 1976) because of the erratic discharges and high tidal range. Since the mid 19th century, 73 per cent of the delta's area has been converted to agriculture, necessitating 1800 km of levees (Logan, 1990).

The McCormack–Williamson Tract (MWT) is uniquely located at the head of the delta downstream from the confluence of the Cosumnes and Mokelumne rivers and adjacent to the Sacramento River (Figure 1). The Cosumnes River is the only major river flowing out of the Sierra Nevada whose mainstem is undammed. MWT is ~650 ha in area and is bordered by the Mokelumne River to the east, Snodgrass Slough to the west, and artificial dredge channels to the north and northeast. Historic maps show that MWT supported freshwater wetland in the early 20th century (United States Geological Survey, 1911). The wetland was likely tidal, as the adjacent channels are presently tidal for several miles upstream. Subsequently, the tract was leveed, drained, and converted into agricultural land. After drainage, MWT and other delta islands experienced subsidence as surface organic sediment was oxidized and decomposed (Rojstaczer *et al*., 1991).

Band (1998) and Florsheim and Mount (2003) indicate that tectonic subsidence around the delta is somewhere between 0·15 and 0·5 mm per year. The primary sea-level rise curve for the region by Atwater (1979) did not account for tectonic subsidence or local compaction, but acknowledges that compaction of peat deposits in the delta could influence subsidence rates. In modern times farmed peatlands further downstream from MWT have

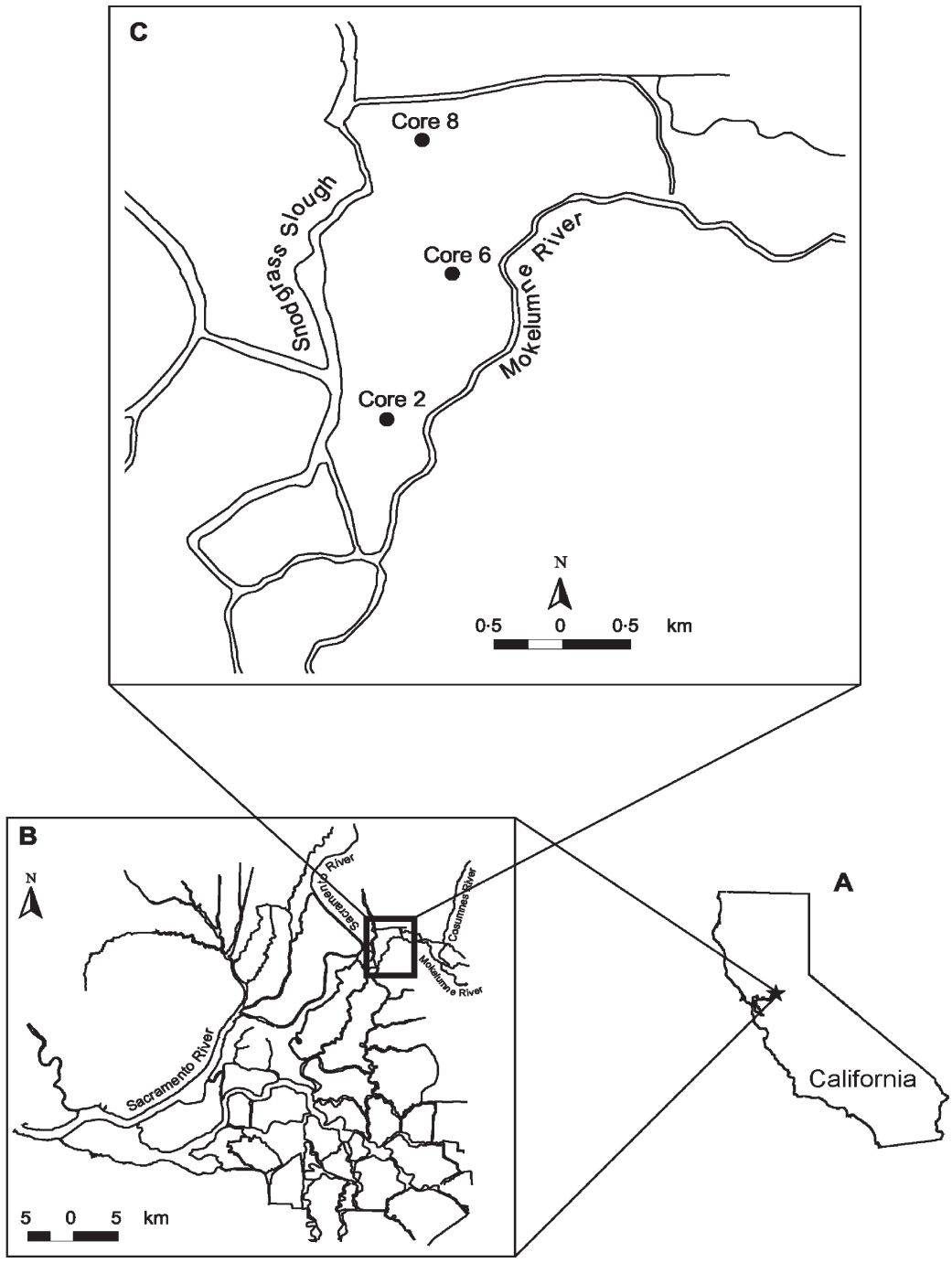

Figure 1. (A) Regional location map showing the location of the study site (star). (B) Map of the Sacramento–San Joaquin Delta. The McCormack–Williamson tract is located within the box at 38·25° N and 121·49° W. (C) Core locations on the McCormack–Williamson tract

subsided at a rate of 7·5 cm per year due to surficial decomposition and deflation. Another factor that could cause subsidence in the delta and on the floodplain is underlying sediment compaction caused by aggradation. However, because the long-term rates and amount of subsidence are not precisely known we do not adjust our data to account for subsidence but rather note that subsidence has and is occurring in the delta region.

The general climate in the MWT region is Mediterranean, with cool, wet winters and hot, dry summers. Climate normals for the years 1961–1990 from Lodi, a town located ~15 km southeast of MWT, record an average minimum temperature of 2·3 °C in December and an average maximum temperature of 33 °C in July. Monthly precipitation varies from an average of 1·8 mm in July to 80·8 mm in January. Annual precipitation averages 434 mm. A cool 'delta breeze' typically blows inland from the estuary during the summer, cooling night-time temperatures. Winter precipitation is predominately rain, though in the high Sierra Nevada the main form of precipitation is snow. In the spring, snowmelt is retained in reservoirs for summer use, though historically it created widespread lowland flooding.

The little riparian vegetation that exists at MWT is largely located along the levees. Scientific nomenclature follows that of Hickman (1996). The most common trees include *Quercus lobata* (valley oak), *Populus fremontii* (Fremont cottonwood), *Platanum racemosa* (western sycamore), *Acer negundo* (box elder), *Fraxinus latifolia* (Oregon ash), and *Alnus rhombifolia* (white alder). Atwater (1980) also recorded the presence of *Cornus stolonifera* (creek dogwood). *Vitis californica* (California grape) grows on many trees. Common shrubs include *Rosa californica* (California rose), *Rubus discolor* (himalayaberry), and several species of *Salix*. *Cephalanthus occidentalis* (bottonbush) was noted close to the channels and *Chenopodium ambrosioides* (Mexican tea) occupies open disturbed sites. Nearby wetlands consist predominately of *Scirpus acutus* (common tule).

METHODS

To characterize the geomorphic relations and paleoenvironmental conditions on MWT, three long sediment cores (MWT-2, MWT-6, and MWT-8) were collected along the longitudinal axis of the tract (Figure 1). MWT-2 is located near the southern tip where the elevation is −30 cm relative to the NGVD (1929 National Geodetic Vertical Datum) mean sea-level position. MWT-6 is centrally located on MWT and is +30 cm NGVD. MWT-8 is located in the northwest section of MWT and is also +30 cm NGVD.

The cores were collected incrementally using a Geoprobe drilling rig (Figure 2) with direct push and dual-tube sampling technology that enables the cores to be recovered in 1·22 m plastic liners. Sediment compaction or expansion during coring was measured on a section-by-section basis as the difference between pushed

Figure 2. The Geoprobe coring rig used to collect the sediment cores. Note the duel tubes in the ground (arrow). The outer tube ensures that the coring hole does not collapse and that each coring drive is vertically aligned with the previous drive. The smaller inner tube is attached to the core head

Table I. AMS radiocarbon dates from cores MWT-2, MWT-6, and MWT-8 with 1 standard deviation statistics. The radiocarbon dates were converted into median calendar ages using a calibration program (Stuiver and Reimer, 1993). The median calendar ages were then rounded to the nearest 500-year interval to reflect the precision of the age–depth model

Sample number	Site	Material	Depth (cm)	Conventional ^{14}C date (ybp)	Median calendar age (cal BP)	Rounded age (cal BP)
Beta-160022	MWT-2	Organic sediment	420–430	20 160 ± 170	23 860	24 000
Beta-160023	MWT-2	Organic sediment	1 060–1 070	12 420 ± 90	14 670	14 500
Beta-160024	MWT-2	Organic sediment	1 070–1 080	23 550 ± 210	N/A	N/A
Beta-151650	MWT-2	Organic sediment	1 260–1 270	40 100 ± 1 010	N/A	N/A
Beta-160025	MWT-6	Organic sediment	370–380	5 730 ± 50	6 530	6 500
Beta-160026	MWT-6	Organic sediment	690–700	7 700 ± 60	8 480	8 500
Beta-151651	MWT-6	Organic sediment	1 290–1 300	8 630 ± 40	9 560	9 500
Beta-160027	MWT-8	Organic sediment	80–90	710 ± 40	665	500
Beta-160028	MWT-8	Peat	540–550	4 290 ± 50	4 860	5 000
Beta-151652	MWT-8	Wood in peat	1 040–1 050	4 970 ± 50	5 700	5 500
Beta-160029	MWT-8	Organic sediment	1 210–1 220	15 890 ± 100	18 970	19 000
Inferred-1	MWT-2	N/A	367	3 100	3 340	3 500
Inferred-2	MWT-2	N/A	795	7 845	8 610	8 500

distance and actual core length. Core sections were stored in a refrigerated room at ~4 °C. To split a core section in the laboratory, the core liner was first cut lengthwise using a circular saw on opposite sides and then a nylon string was passed down the core section between the cuts to yield two halves. Any smeared sediment was carefully scraped off the exposed sediment surface in a horizontal fashion using a plastic spatula. Subsequently, core lithologies were visually described and plastic u-channels were pushed longitudinally into one half of each core section to retrieve samples for magnetic susceptibility. Next, cores were subsampled in 10 cm intervals and subsamples were placed in labeled plastic bags for cold storage and later analyses. Selected organic samples were sent to Beta Analytic Inc., University Branch, Miami, Florida, for accelerator mass spectrometry (AMS) radiocarbon dating (Table I). The radiocarbon dates were converted to calendar ages using a calibration program developed by Stuiver and Reimer (1993). Non-linear radiocarbon and calendar year age–depth models were developed by fitting a locally weighted function to the reported dates. Vertical accretion (cm per year), sedimentation rates (g cm^{-2} per year), and charcoal flux were determined using the calendar age–depth model.

In order to obtain a cross-comparison of the cores to interpret geomorphic dynamics, each core's stratigraphy was determined using both visual and analytical methods, and then a statistical clustering algorithm was applied to the data to objectively zone each core. Analysis of sediment cores involved a multi-proxy approach in which standard physical, chemical, and paleoecological parameters were quantified. Sediment characteristics such as bulk density, loss-on-ignition (LOI), and magnetic susceptibility were measured for all core subsamples. Sediment bulk density (g cm^{-3}) was determined for the cores by weighing a subsample and measuring its volumetric displacement in a 50 ml graduated cylinder. Percentage organic and inorganic matter was obtained by LOI. Samples were weighed wet, dried overnight at 60 °C, weighed dry, combusted for 6 h at 600 °C in a muffle furnace, and reweighed. The difference between sample wet and dry mass is the water content and the difference between sample dry and post-combustion mass is the organic matter content. Magnetic susceptibility was measured for 30 s in 1 cm intervals down-core using a Bartington MS2 magnetometer and was adjusted for compaction. U-channels were then stored as archival sediment records at 4 °C.

Percentages of sands versus fines (silt and clay) were determined for each sample using methods adapted from Folk (1974). Organics were removed using 30 per cent H_2O_2 (Black, 1965; Pasternack and Brush, 2002). Next, samples were suspended in 500 ml 0·5 per cent sodium metaphosphate ($(NaPO_3)_x{\cdot}Na_2O$) to fully disaggregate particles and passed through a 63 μm sieve to separate sands from fines. Sands were collected, rinsed with distilled water, dried, and weighed to determine total mass of sand. The fines suspended in the sodium metaphosphate were retained after wet separation and subsequently transferred into a graduated cylinder to determine total suspended volume. The fines were then transferred into a plastic bottle and vigorously shaken to homogenize the suspension. A 20 ml subsample was pipetted into a weighing dish, dried, and weighed.

Subsample mass was calculated as the dry mass minus the mass of 20 ml of 0·5 per cent sodium metaphosphate. The total mass of fines was calculated by multiplying the mass of the dry fines in the 20 ml pipetted subsample by the volume of the sample divided by the subsample volume. Based on the total mass of measured sand and fines, the percentages of each fraction were calculated.

Even though aluminum is not commonly used to directly assess geomorphic dynamics, its abundance and variability in siliciclastic sediment makes it very useful in identifying strata that may not be visually evident. Sediment samples for Al analysis were dried, ground, and passed through a 0·177 mm sieve to obtain the fine fraction. Next, they were treated with hot concentrated nitric acid to destroy organic matter and oxidized sulfide material and then added to concentrated hydrochloric acid (three times the volume of the nitric acid) to digest the material. After digestion, sample solutions were analyzed using inductively coupled argon plasma with atomic emission spectroscopy. Because sediment digestion was only 'partial' for Al, a reference soil sample (San Joaquin Soil Standard Reference Material 2709) from the National Institute of Standards and Technology was also analyzed for Al using the same procedure. The difference between the measured and known element concentrations for the reference standard was the non-leachable fraction. Because the reference material came from a field near the study site, its texture, composition, and thus leachable fraction should be very similar to those for samples from the sediment cores. For easier up-core comparison, Al concentrations were normalized by a basal average concentration representing an initial state from which up-core changes could be assessed on a simplified scale. Samples from the bottom meter of each core were used to obtain the basal average.

Because observers can easily bias grain size and color information in determining core stratification, cluster-based zoning using quantitative sediment properties was used to promote objective core interpretation. The cores were divided into zones and subzones using a stratigraphically constrained cluster diagram that was based on values of LOI, fine sediment percentage, magnetic susceptibility, and normalized Al concentrations. These variables were selected for cluster analysis because they are continuous throughout the cores and are not modified down-core by compaction. The core zones are used throughout the text to describe, compare, and contrast the cores and core variables.

Additional information on the paleoenvironmental history of the upper delta was obtained from pollen and charcoal analysis. Pollen preparation followed standard procedures (Moore *et al*., 1991) and the samples were spiked with *Lycopodium* tablets containing 10 679 ± 953 spores (Batch Number 938934). The pollen and spores were counted using a Nikon Eclipse E200 microscope at 400× magnification and identified with reference to pollen floras (Moore *et al*., 1991) and the University of California Museum of Paleontology Pollen Reference Collection. Pollen counts were converted to percentages using a total of all pollen and spores.

Charcoal fragments were retrieved by sieving 1 cm^3 of homogenized sediment through a 150 μm sieve (Brown and Hebda, 2002a). The sediment was homogenized to ensure that the charcoal extract was representative of the subsample. The residue that did not pass through the sieve was suspended in water in a gridded Petri dish and examined using a dissecting microscope at 40× magnification. Black fragments that were brittle and opaque with sub-metallic lustre and cellular structures were counted as charcoal (Sander and Gee, 1990). Charcoal flux (fragments cm^{-2} per year) was obtained by multiplying the number of fragments per 1 cm^3 of sediment (fragments cm^{-3}) by the sedimentation rate (cm per year).

RESULTS

The majority of the results and interpretations are dependent on a robust age–depth model based on the radiocarbon and calendar chronologies, so that is described first in detail. Once the chronologies are established, then the quantitative stratigraphic histories of each core are presented. Next, cross-core and down-core relationships among sediment variables are reported. Lastly, the age–depth model is reassessed using the established relationships between variables.

Age-depth models

For the time-scale of interest in this contribution and the nature of the materials collected as part of this investigation, there is no definitive dating approach that would yield an absolutely accurate representation of chronology. Therefore we employed the widely used radiocarbon dating method (e.g. Hudson-Edwards *et al*.,

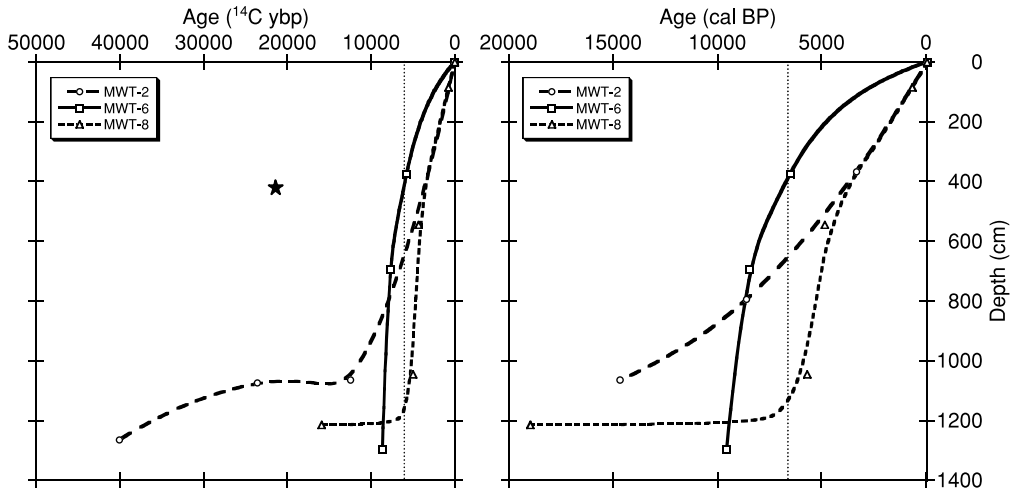

Figure 3. Radiocarbon (^{14}C ybp) and calendar (cal BP) year age–depth models. The star represents the discarded date inversion. The vertical dotted line represents the 5700 ^{14}C ybp and 6500 cal BP mark that is discussed in the text

1999; Constantine *et al*., 2003). Of the 11 AMS radiocarbon dates obtained for the cores (Table I), only one from MWT-2 (Beta-160022) shows date inversion (Figure 3). This sample derives from a shallow level in MWT-2, but its date is very old and inconsistent with the other dates in that core and the other cores. The age of the material is thought to be too old due to long-term storage and eventual reworking of old carbon from upstream floodplains. The two bottom radiocarbon dates from MWT-2 are old and do not yield valid calibration ages. In consequence, we have elected to present two age–depth models: a conventional radiocarbon model and a calibrated calendar year model (Figure 3). The radiocarbon age–depth model for MWT-2 consists of three dates whereas the corresponding calendar chronology is reduced to one reliable date. Additional radiocarbon samples were not obtained for MWT-2 because visible organic matter such as wood fragments were not observed at any other levels apart from those already dated. The resulting calendar age–depth model for MWT-2 is a linear model that likely does not accurately reflect patterns of past sedimentation. Subsequently, an alternate and preferred calendar chronology, consisting of three dates (one measured and two inferred), was developed for MWT-2 using the radiocarbon age–depth model. The inferred dates were selected as the points of cross-over between MWT-2 and the other cores in the radiocarbon age–depth model. The inferred radiocarbon dates were then converted to calendar years (Table I) and a new MWT-2 calendar age–depth model developed. All ensuing core calculations, such as accretion and sedimentation rates, were based on the MWT-6 and MWT-8 calendar age–depth models as well as the inferred model for MWT-2 respectively.

The most believable and perhaps reliable radiocarbon dates in the age–depth models are from the organic (peat and wood-in-peat) deposits in MWT-8 at 1040–1050 and 540–550 cm depth because these ages are derived from *in situ* wetland sediment that was deposited in a stable environment. In MWT-2, the dates at 1065 and 1075 cm depth are also thought to be correct because they suggest extremely slow sedimentation or the existence a hiatus across a sharp lithological boundary that corresponds to late-Wisconsin glaciation in California (Bischoff and Cummins, 2001). The confidence in the remaining dates is intermediate because of possible temporary upstream sediment and carbon storage in hillslope colluvium, floodplains, or terraces that creates a gap between organism death and final deposition in the delta. The basal date in MWT-2 must be viewed with caution since it is near the limit of radiocarbon detection.

MWT-2 stratigraphy

The stratigraphically constrained cluster analysis identified six zones (MWT2-1 to MWT2-6) in the MWT-2 core (Table II, Figure 4). Note that the chronology in MWT-2 shifts from radiocarbon years to calendar years because the oldest dates extended beyond the radiocarbon–calendar calibration curve and could not be converted

Table II. Core characteristics where LOI = loss on ignition and MS = magnetic susceptibility. The values presented are zone averages unless a range is specified

Zone	Depth (cm)	Age (cal BP)	Al (%)	Bulk density (g cm^{-3})	LOI	Fines (%)	MS ($\times 10^{-5}$ SI units)	Pollen	Charcoal (fragments cm^{-2} per year)
MWT2-6	0–100	0–800	3·1	1·7	5·9	94	16	Absent	0·3
MWT2-5	100–230	800–2 000	2·0	2·2	1·8	59	86	Absent	0
MWT2-4	230–430	2 000–4 000	2·4	2	3·4	77	53	Absent	0
MWT2-3	430–1 010	4 000–13 000	1·5	2·1	1·8	34	54	Absent	0
MWT2-2	1 010–1 140	>13 000	2·3	2·0	3·6	74	63	Absent	0
MWT2-1	1 140–1 325	>13 000	2·4	1·7	4·8	97	178	*Pinus* (15%), *Populus* (2%), *Quercus* (1%), *Lithocarpus* (2%), *Juglans* (2%), TCT (5% at top), Rosaceae (1%), *Salix* (4%), *Alnus* (2%), *Artemisia* (2%), Compositae (20%), Rubiaceae (15%), Poaceae (4%), Chenopodiaceae (1%), trilete ferns (10%), monolete ferns (10%), *Typha* (2%), Cyperaceae (1%), *Isoetes* (1%), *Equisetum* (1%)	0
MWT6-3c	0–140	0–3 800	2·7	1·9	8·3	94	15	rare (*Pinus*, *Populus*, *Alnus*, Asteraceae, *Zea*, Chenopodiaceae, trilete spores)	0
MWT6-3b	140–260	3 800–5 500	2·1	1·9	4·6	63	15	Absent	0·1
MWT6-3a	260–340	5 500–6 200	2·8	1·8	7·7	86	20	Absent	1·3
MWT6-2b	340–520	6 200–7 500	1·8	2·0	2·7	25–69	152	Absent	0–16
MWT6-2a	520–700	7 500–8 500	2·8	1·9	4·8	58–85	152	Absent	0–1·2
MWT6-1	700–1 435	>8 500	1·7	2·2	2·0	11–56	190–580	Absent	0–13
MWT8-5	0–90	0–700	3·2	1·8	6·4	90	63	*Pinus* (12%), *Populus* (5%), *Acer* (1%), *Quercus* (3%), *Lithocarpus* (2%), *Juglans* (2%), *Salix* (1%), *Alnus* (2%), Compositae (15%), Rubiaceae (6%), Umbelliferae (2%), Poaceae (1%), *Zea* (4%), Chenopodiaceae (9%), *Typha* (8%), Cyperaceae (4%), *Nuphar* (1%), *Potamogeton* (1%), *Equisetum* (2%), trilete spores (4%)	1·0
MWT8-4	90–480	700–4 100	2·7	1·7	5·5	92	24	*Pinus* (23%), *Quercus* (9%), *Lithocarpus* (6%), *Juglans* (1%), *Salix* (9%), *Myrica* (3%), *Alnus* (2%), Compositae (5%), Rubiaceae (14%), Poaceae (1%), Chenopodiaceae (2%), *Typha* (4%), Cyperaceae (3%), monolete spores (1%), trilete spores (4%)	0·6
MWT8-3	480–850	4 100–5 400	3·0	1·4	6·1–32·1	95	10	*Pinus* (6%), *Populus* (1%), *Quercus* (6%), *Lithocarpus* (14%)	0–54
MWT8-2	850–1 125	5 400–6 600	1·9	2·2	2·0	35	270	Absent	0–0·4
MWT8-1	1 125–1 220	>6 600	1·7	2·0	3·9	60	110	Absent	0

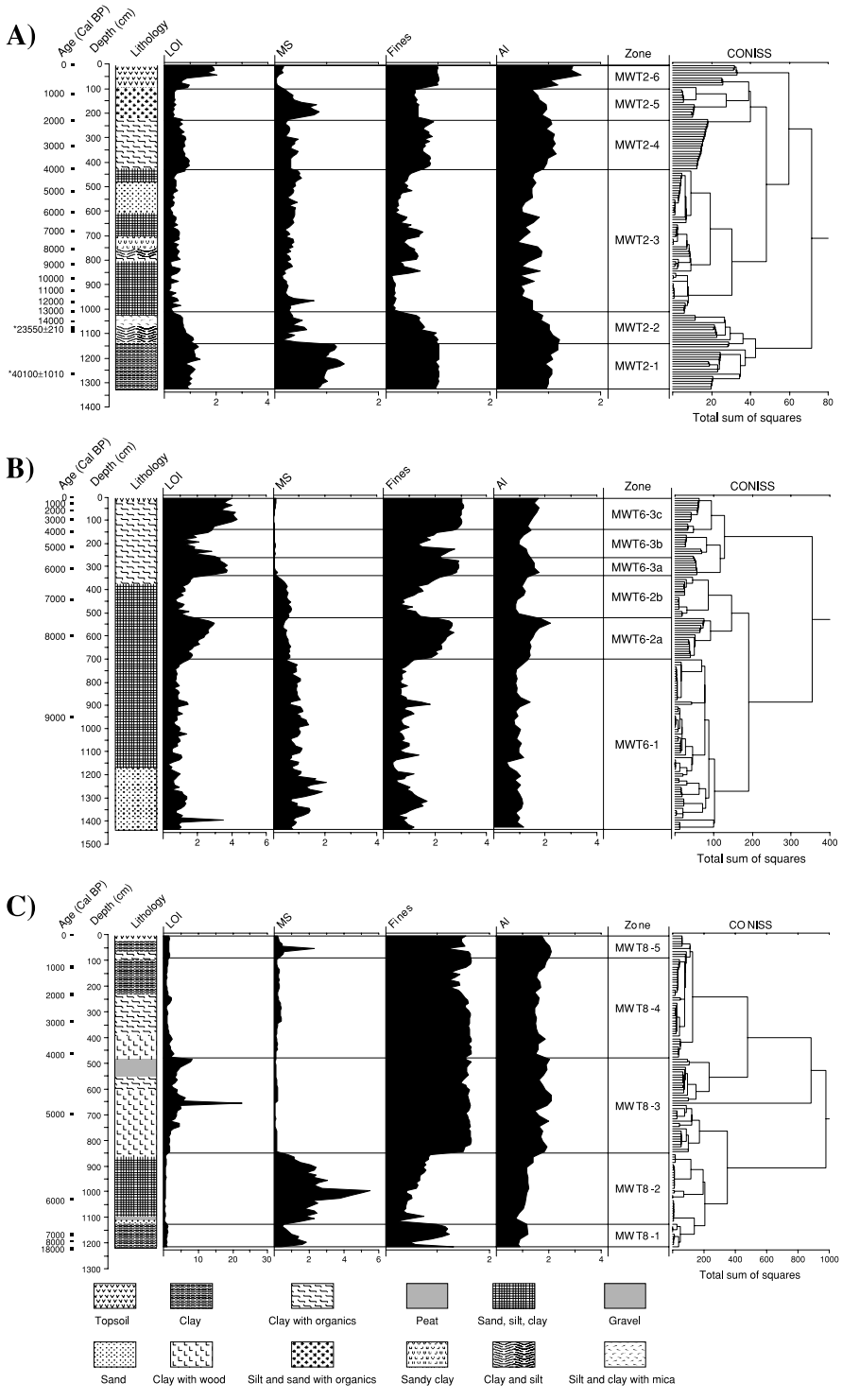

Figure 4. Stratigraphically constrained cluster diagrams for (A) MWT-2, (B) MWT-6, and (C) MWT-8. The diagrams have been normalized using the average values from the bottom 1 m. Therefore, a value of 1 reflects average basal conditions, >1 reflects enrichment, and <1 reflects depletion. Differences between the visual lithology and the cluster analysis confirm the utility of the objective approach. The two basal dates in MWT-2 are in radiocarbon years whereas all remaining ages are in calendar years. LOI, loss on ignition; MS, magnetic susceptibility

into calendar ages. MWT-2 is 1330 cm long and begins in gray clay from 1330–1135 cm that was deposited between roughly >40 000 and 29 000 radiocarbon years before present (^{14}C ybp). Alternating bands of green silt and clay occur from 1135–1070 cm depth and span the interval from approximately 29 000 to 24 000 ^{14}C ybp. The radiocarbon chronology indicates that an interval of extremely slow sedimentation or a hiatus exists at 1070 cm depth and spans approximately 11 000 ^{14}C years. Silt with visible mica flakes was deposited after about 14 500 calendar years before present (cal BP) from 1070–1026 cm depth. Coarse sand with layers of silt and clay from 1026–800 cm is followed by a layer of beige clay with organic fragments from 800–788 cm depth. These units were deposited between roughly 13 500 and 8500 cal BP. Olive silt occurs from 788–755 cm depth. Greenish-grey sandy-clay is recorded from 755–700 cm depth. Alternating layers of gray silt and sand noted between 700 and 607 cm depth are followed by alternating layers of gray and red-brown sand between 607 and 482 cm depth. Mottled sand, silt, and clay are observed between 482 and 427 cm. The mottles are typically dark gray and brown and 1–2 mm in size. The units from 755–427 cm depth were deposited between about 8000 and 4000 cal BP. Clays containing concretions and organics that were deposited between 4000 and 1900 cal BP (427–220 cm) are interrupted by a thin sand layer at 307–299 cm depth. Sand and silt with organic fragments are present from 220–96 cm. Clays with high organic content occur between 96 and 0 cm depth.

MWT-6 stratigraphy

Three zones were identified for MWT-6 (MWT6-1 to MWT6-3; Table II, Figure 4). Zones MWT6-2 and MWT6-3 are subdivided into two (MWT6-2a and MWT6-2b) and three (MWT6-3a to MWT6-3c) subzones respectively. MWT-6 is 1440 cm long and begins in alternating fine, medium, and coarse red-brown sands with wood fragments from 1440–1170 cm. These sands were deposited before >9500 cal BP. Alternating bands of sand and silt occur between 1170–376 cm depth from about 9500–6500 cal BP, with less sand between roughly 500 and 700 cm depth. Clay with organic fragments near the bottom and 1–2 mm dark gray-brown mottles near the top occur from 376–8 cm depth. Organic topsoil is noted from 8–0 cm depth.

MWT-8 stratigraphy

Five zones are identified in MWT-8 (MWT8-1 to MWT8-5; Table II, Figure 4). MWT-8 is 1220 cm long and begins in green-blue clay from 1220–1121 cm that was deposited before 16 000 ^{14}C ybp to about 6500 cal BP. A coarse sand unit between 1121 and 1105 cm is followed by a thin layer of gravel from 1105–1100 cm depth. Alternating sand and clay units are visible from 1100–866 cm depth. The units containing sand from 1121–866 cm were deposited between approximately 6500 and 5500 cal BP, with the gravel being laid down at about 6400 cal BP. Clay with wood and other organic fragments occurs between 5500 and 4700 cal BP (866–607 cm depth) with large wood fragments occurring at 662 and 633 cm. Organic-rich clay from 607–550 cm yields to peat between 550 and 482 cm depth at about 4500 cal BP. The organic-rich clay recurs at about 4100 cal BP and comprises the core between 482 and 399 cm depth. Wood fragments are noted at 435–431 and 399–395 cm depth. Clay with organic fragments from 395–231 cm is replaced by mottled clay from 231–94 cm. Alternating organic and mottled clay units occur between 94 and 65 cm depth. Clay is again noted between 65 and 20 cm with imbedded gravel and pebbles at 58–52 cm. The clays between 395 and 20 cm depth were deposited between 3500 and 100 cal BP and the gravels laid down at about 400 cal BP. Organic topsoil occurs from 20–0 cm depth.

Vertical accretion and sedimentation rate trends

The established radiocarbon and calendar chronologies permit calculation of down-core vertical accretion (cm per year) and associated sedimentation (g cm^{-2} per year) rates and examination of their trends (Figure 5). The entire MWT-2 core is characterized by relatively slow rates of vertical accretion. The rate increased up-core over a 15 000-year period from a basal low of 0·03 cm per year to a high of 0·12 cm per year. In contrast, accretion rates in MWT-6 are initially high (ca. 0·7 cm per year) at about 9500 cal BP, but decrease sharply through time in two stages to ~0·05 cm per year. Extremely slow accretion in the bottom of MWT-8 is followed by a marked increase during the mid-Holocene with peak rates of ~0·4 cm per year occurring at 5500–5000 cal BP. Slower accretion rates of ~0·1 cm per year recur in the late-Holocene. During the last 3500 years, MWT-2 and MWT-8 show remarkably similar rates of accretion. However, the age–depth models also reveal that discrepancies exist between the cores in terms of sediment age and depth of deposition. For example, the calendar year

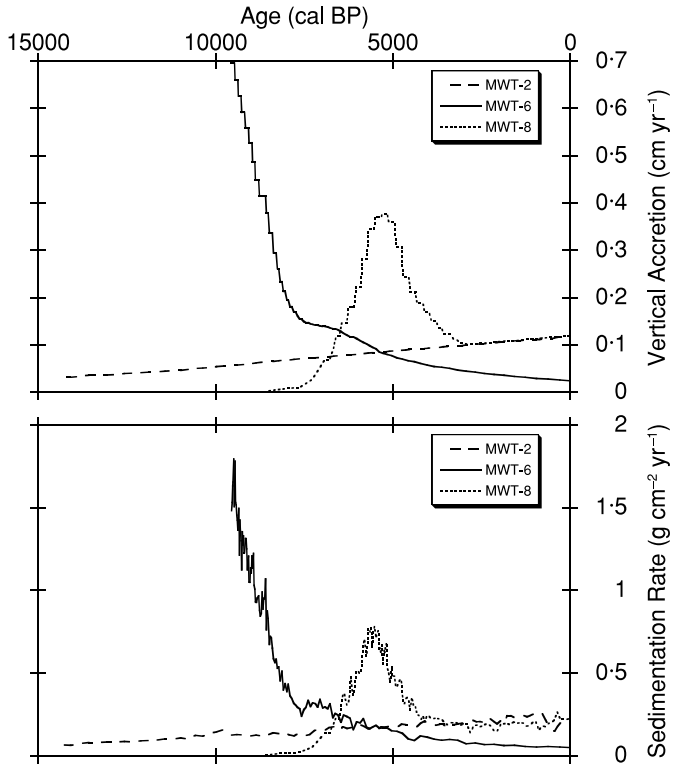

Figure 5. Trends in vertical accretion and sedimentation through time

model suggests that at 6500 cal BP the surface elevations of MWT-6, 2, and 8 were roughly 375, 650, and 1100 cm below the present surface respectively (Figure 3). The radiocarbon model similarly records this discrepancy at 5000 ^{14}C ybp. The possibility of this steep a gradient is discussed below in light of the multiple proxies and several explanations are examined.

Temporal trends in sedimentation rates parallel those of vertical accretion to some extent (Figure 5), given the narrow range of observed bulk densities in each core (Table II). MWT-2 shows little down-core variability, with sedimentation rates ranging between ~0·05 g cm^{-2} per year at the bottom of the core to 0·2 g cm^{-2} per year at the top. A high sedimentation rate of 1·5 g cm^{-2} per year is initially observed in the bottom of MWT-6 at 9500 cal BP, after which values decrease noticeably until about 8000 cal BP. More gradual change is noted between 8000 cal BP and the present as sedimentation rate decreases from 0·5 to 0·05 g cm^{-2} per year respectively. In contrast, the sedimentation rate is initially very low in MWT-8, with basal values ranging between 0·01 and 0·1 g cm^{-2} per year. In the mid-Holocene, sedimentation rates increase to a maximum of 0·8 g cm^{-2} per year at 5500 cal BP and then decrease to 0·2 g cm^{-2} per year by 4000 cal BP. Between 4000 cal BP and the present, sedimentation hovers around 0·2 g cm^{-2} per year.

Grain-size relations with accretion and sedimentation

Vertical accretion and sedimentation rates at MWT are significantly higher and more variable during coarse sediment deposition (Figure 6). MWT-6 and MWT-8 both show high rates of accretion and sedimentation when fines constitute less than 50 per cent of the total sediment being deposited. When fines are greater than 50 per cent, both accretion and sedimentation are profoundly slower. No threshold or trend between grain size and accretion or sedimentation rates is evident in MWT-2. Low rates of sedimentation characterize MWT-2 regardless of fine content. The wetland deposit (MWT8-3 and bottom of MWT8-4) is characterized by a high percentage of fines and by intermediate accretion and sedimentation values that are less than those for coarse inorganic sediment but generally greater than those for fine inorganic sediment.

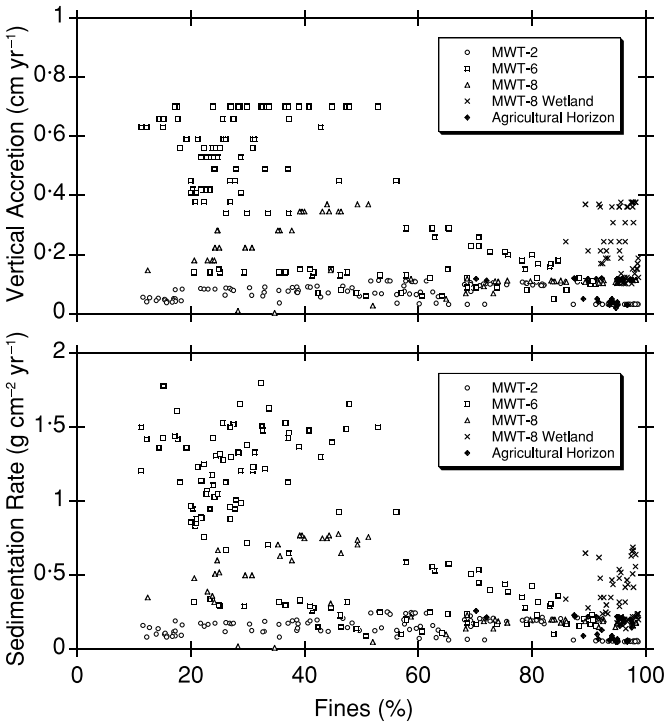

Figure 6. Cross-core relations between fines, vertical accretion, and sedimentation rates

Comparison of the grain-size data among cores shows that while a variety of sediments were deposited on the MWT floodplain through time, there are recognizable patterns across the tract (Figure 7). MWT-2 and MWT-8 are characterized by fine-grained sediment below 1100 cm depth that is overlain by coarser grained deposits. Meanwhile, the basal sediments in MWT-6 are generally coarse-grained. Above the coarse-grained units in MWT-2 and MWT-6, there are strong fluctuations in grain size superimposed on an overall trend of upward fining. MWT-2 records grain-size fluctuations and general upward fining starting at about 13 000 cal BP. In contrast, MWT-6, while of similar length, is of shorter duration and records grain-size fluctuations and upward fining starting at a minimum age of about 9500 cal BP. The fluctuations are marked by three periods of fine-sediment deposition and two periods of coarse-sediment deposition. In MWT-2, the first episode of fine deposition was marked by two intermittent periods of coarsening. The thickness of each fine and coarse layer is greater in MWT-2 than MWT-6. MWT-8 differs from MWT-2 and -6 in that it predominately consists of fine-grained sediment above the lower coarse unit, though perhaps some correlation can be made between the coarser units in MWT-2 and MWT-8 at 6500–5500 and 2000–1000 cal BP.

Sources and rates of organic deposition

At MWT, organic content does not diminish as a function of depth in response to duration of potential decomposition (Figure 4), but instead shows a strong, direct linear relationship to fine sediment content in all cores (Figure 8). *In situ* organic material stemming from biomass accumulation under either reducing freshwater wetland or agricultural conditions is easily identifiable visually and by relatively high LOI values and the highest fine sediment contents. For example, the *in situ* organic layers in MWT-8 (zones MWT8-3 and bottom of MWT8-4) consist of peat and fine sediment with very high organic matter content compared to fine floodplain sediment. The organic matter in peat consists of visible plant fragments, whereas the organic matter in floodplain sediment is microscopic and may include a balance of terrestrial versus aquatic (algal and microbial) sources (Wolfe *et al*., 2002).

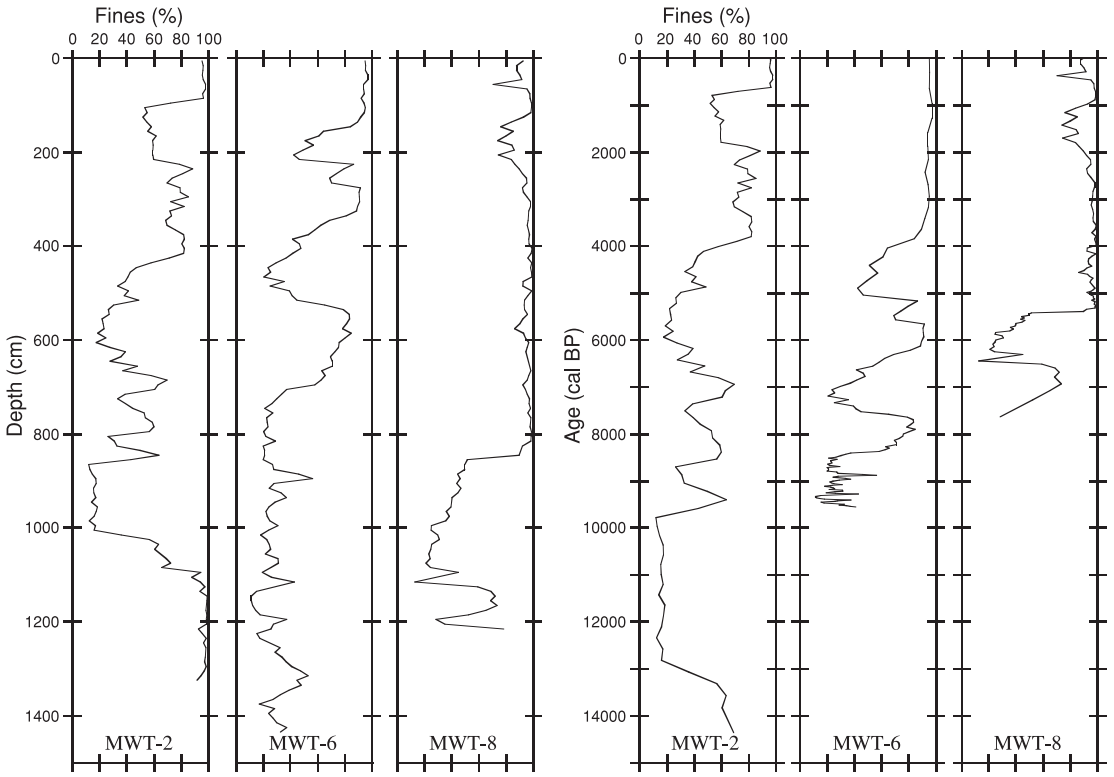

Figure 7. Percentage fines variation with depth and calendar age. The two hydrological domains in the cores are the coarse–fine fluctuations superimposed on general upward fining. The core names are shown at the bottom of each panel

When the *in situ* organic and peat deposits in MWT8-3 and bottom of MWT8-4 related to wetland development and surficial core intervals impacted by agricultural activity (i.e., zones MWT2-6 and MWT6-4c) are excluded from analysis due to their known and distinct origin, the correlation between organic content and fine content for each core is statistically significant above the 99 per cent confidence level, with R values ranging from 0·78 to 0·87. The curve representing all of the combined data has a slope and y-intercept that matches MWT-8 almost perfectly. The MWT-8 and MWT-2 curves have similar slopes, whereas MWT-6 has a slightly greater slope. Based on the sedimentation monitoring research and associated endmember mixing modeling on a tidal freshwater delta reported by Knight and Pasternack (2000), the observed relationship is indicative of mixing between two distinct sedimentary endmembers: landscape wash load that is predominately fine with higher organic content and channel bed material load that is predominately sandy with low organic content. Depth intervals with intermediate amounts of fine sediment and organic content represent linear mixtures of the two sources, as the observed relationships are all linear.

Extrapolation of the regression lines to 100 per cent fines indicates that the organic content of the fine-sediment endmember, which primarily derives from hillslope sources, is about 5·5 per cent when all core data is considered but ranging between 4·4 and 7·9 per cent for the individual cores. Similarly, extrapolation of the lines to 0 per cent fines yields an organic content of 0·5 per cent and a range of 0·1–0·5 per cent for the coarse-sediment endmember, which derives from channel bed material. In contrast, the wetlands in MWT8-3 and the bottom of MWT8-4 typically contain >95 per cent fines though this value ranges between 86 and 99 per cent. The organic content in these wetlands is between 5 and 32 per cent, with the organic rich clay deposits ranging between 5 and 19 per cent and the peat ranging between 15 and 32 per cent. The sedimentation rate for wash load sediment consisting of >80 per cent fines and about 5 per cent organic matter ranges between <0·1 and 0·3 g cm^{-2} per year with a very small contribution to that made by the organics (Figures 6 and 8). Thus, *in situ* biogenic accumulation of sediment is a negligible component of overall vertical accretion. In contrast, wetlands

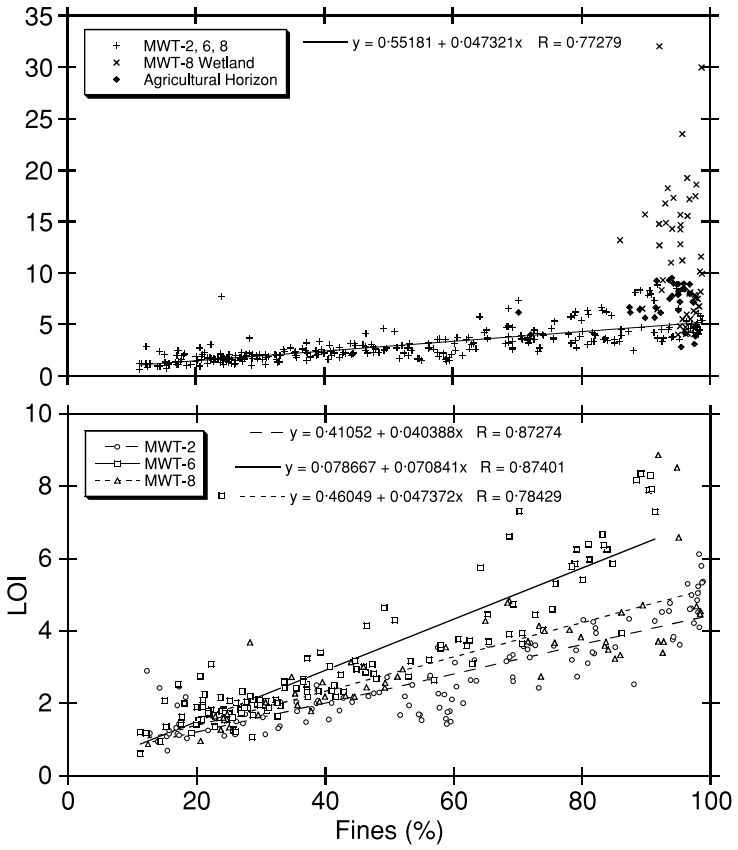

Figure 8. Linear relationship between fine sediment (silt and clay) and particulate organic matter (LOI). The top panel contrasts floodplain samples from all cores with wetland and agricultural samples. The bottom shows the relationship for each individual core. Agricultural and wetland samples are not included in the bottom panel

contain only slightly more fines and yet have noticeably higher sedimentation rates that range between 0·2 and 0·7 g cm^{-2} per year, of which 0·05–0·2 g cm^{-2} is directly due to organic accumulation. The wash load fraction having comparable sedimentation rates to that of the wetlands is typically much coarser grained, containing between 20 and 80 per cent coarse sediment.

Paleoenvironmental indicators

Magnetic susceptibility also shows a relationship to fine-sediment content, though it is more complex (Figure 9). In general, coarse sediment has a higher magnetic susceptibility compared to fine sediment. This relationship is related to the transport and deposition of dense ferromagnetic minerals (i.e., magnetite) with coarser sediment (Berry and Mason, 1983). Indeed, examination of the sediment under a dissecting microscope reveals that black, opaque, magnetic minerals are more common in the medium and coarse sand units compared to the fine sediment.

MWT-6 and MWT-8 illustrate this relationship well with intervals of >50 per cent fine content having magnetic susceptibility $<200 \times 10^{-5}$ SI units and intervals of <50 per cent fines having magnetic susceptibility between 200 and 600×10^{-5} SI units. MWT-2, on the other hand, shows no general relationship between grain size and magnetic susceptibility, with coarse sediments having relatively low magnetic susceptibility values and some fine sediments having elevated values (Table II; Figure 4). The only other deviation to this pattern is observed in zone MWT6-3b, where there are almost no variations in magnetic susceptibility regardless of fine content. Perhaps the low values in the coarse sediment in MWT-2 are related to post-depositional diagenesis of

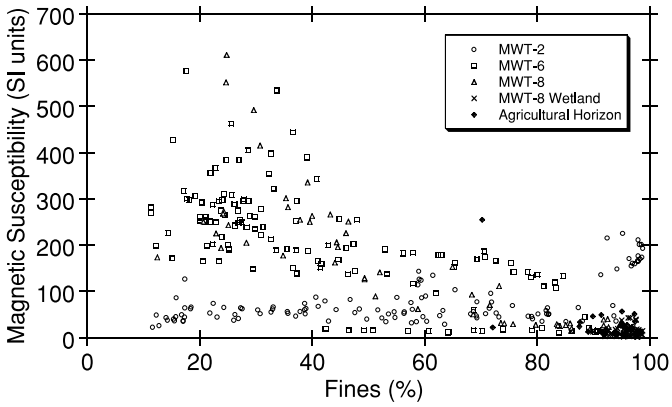

Figure 9. Scatter diagram of fines versus magnetic susceptibility. The cluster of samples around 200 SI units and >95 per cent fines are from MWT2-1

the magnetic minerals. Magnetite can dissolve during diagenesis in contact with reducing or acidic pore fluid, resulting in a loss or reduction of the magnetic susceptibility signal (Singer *et al*., 1996). MWT-2 is located at the southern end of MWT at a lower elevation compared to cores 6 and 8 (Figure 1). In consequence, MWT-2 experienced greater submergence and related anaerobic conditions, which likely enhanced the reduction and leaching of iron from the system at this site. This process could account for the lower overall magnetic susceptibility observed in MWT-2 coupled with the lack of a relationship between grain size and magnetic susceptibility. The low magnetic susceptibility from the wetlands in MWT8-3 supports this interpretation because the wetland sediment accumulated under similar anaerobic conditions.

Examination of the pollen and spores (herein pollen) in MWT cores shows that most of the grains are small, roughly equivalent in size to silt. Pollen grains are observed in some core zones but not in others (Table II) and such spotted distribution may be related to the different types of processes operating on the floodplain (Catto, 1985; Fall, 1987). Some zones are poor in pollen because they are dominated by coarse sediment that was deposited during higher velocity conditions that kept fine sediment and hydraulically equivalent pollen grains in suspension. In addition, the coarse-grained deposits would have experienced greater mechanical breakdown of pollen as well as increased post-depositional oxidation of the grains (Havinga, 1967; Brooks and Elsik, 1974; Holloway, 1989; Campbell, 1991). Beuning *et al*. (1997) similarly noted that the lack of sporopollenin microfossils in subaerially exposed sediments was caused by strong oxidizing conditions. Therefore, we posit that fine-grained units should contain more pollen compared to coarse-grained deposits. Pollen is present in non-agricultural zones MWT2-1, MWT8-3, and MWT8-4. The sediment in MWT2-1 averages 97 per cent silt and clay, suggesting that the pollen in this zone was transported and deposited with fine sediment. Zones MWT8-3 and MWT8-4 are characterized by >95 and >92 per cent fines respectively, suggesting that the pollen was transported fluvially with the fine component. The remaining zones that contain abundant fines (i.e. >90 per cent) occur at the top of the cores in the agricultural horizons. MWT6-3c and MWT8-5 record the presence of some pollen, whereas no pollen was noted in MWT2-6. It is hypothesized that the reduced concentration of pollen in the uppermost sediment is related to three factors. First, the crops that are grown on MWT include tomatoes, corn, and safflower, all of which are angiosperms and generally poor producers of pollen. Second, the surface soils on MWT are intensely harvested, which mechanically degrades the pollen grains. Finally, the soils are well aerated, promoting the chemical (oxidation) degradation of exposed grains. The remaining core zones are void or extremely poor in pollen at the 1–2 cm^3 sampling level. These zones contain between 11 and 86 per cent fines, suggesting that the pollen was either not deposited with these units but rather transported to some other depositional site with the fines or was post-depositionally degraded through oxidation. These data suggest that if pollen extraction is desired from a floodplain then sediment with at least >90 per cent fines should be targeted.

The charcoal records show that fire is not and has not been a disturbance factor on the MWT floodplain, even though floodplain vegetation succession studies show that woody plants (i.e., fuel) colonize the site (Tu, 2000). Charcoal fragments are scare on the MWT and occur intermittently down-core (Table II). The most notable

increase in charcoal through time occurs in zone MWT8-3, with flux values reaching a high of 54 fragments cm^{-2} per year. The lithological and pollen data from MWT-8 suggest that Cyperaceae, likely *Scirpus* (Atwater *et al*., 1979), wetlands developed in the northwest corner of the tract during zone MWT8-3.

Age-model revisited

Because the calendar chronology for MWT-2 is derived from one measured date and two inferred dates, it is worthwhile reassessing the model using the established cross-core relations between grain size and accretion, sedimentation, and magnetic susceptibility. More confidence can be placed in the sections of the age model where these relationships are consistent between cores. Slow accretion and sedimentation rates are noted in coarse sediment from MWT-2 compared to more rapid rates in similarly coarse sediment in MWT-6 and MWT-8. Both accretion and sedimentation are time-dependent, suggesting that perhaps the section of the age–depth model contemporaneous to coarse sediment deposition in MWT-2 is erroneous. Coarse sediment is mainly observed in zone MWT2-3 (Table II; Figure 4), representing the 13 000–4000 cal BP interval and this interval is subsequently viewed with less confidence. Magnetic susceptibility from coarse sediment in MWT-2 is considerably lower compared to coarse sediment from MWT-6 and MWT-8, much like accretion and sedimentation. However, unlike accretion and sedimentation, measurements of magnetic susceptibility are not time-dependent, thus implying that the established age–depth model for MWT-2 may in fact be a suitable model because both time-dependent and time-independent variables are behaving similarly and that perhaps the coarse sediment in MWT-2 is itself anomalous compared to the other cores, though the reasons for this are currently unknown. These observations suggest that the MWT-2 age–depth model is a suitable model and that sections dominated by fines can be viewed with more confidence compared to coarse core sections.

DISCUSSION

The three cores from MWT provide new and important insight into geomorphic processes, flow regime history, and evolution of a floodplain–delta interface from the Central Valley in California. There are few paleoenvironmental investigations from this region because suitable organic deposits are rare and inorganic deposits are often difficult to extract. MWT-2 spans the longest duration (>40 000 ^{14}C ybp) and provides some detail about MWT that cannot be realized from MWT-6 and MWT-8 since they predominately span the Holocene. All three cores contain Holocene records and in combination reveal that the MWT was, and continues to be, a highly dynamic site characterized by lateral channel migration, incision, overbank flooding, reducing wetland development, and a mosaic of habitat types. The following discussion initially focuses on developing a facies model for MWT using sediment grain-size characteristics. Next, time–depth discrepancies in the age model are discussed in light of the established facies model. Finally, the cores are examined temporally and the tract evolution is discussed.

Depositional facies

Even though the MWT cores were taken along the longitudinal gradient of the upper deltaic plain, they do not show a simple trend in grain size that would be associated with tidal or fluvial hydraulic sorting along that gradient. Instead, a complex variety of lithologies and sedimentation rates exist, suggesting that various localized flow regimes have characterized MWT in the past. The general relationship between inorganic clastic sedimentation and fine content on MWT suggests that coarse sediments are reflective of channel or near-channel deposits since sediments near river deposits typically have greater sedimentation rates compared to those deposited distally on the floodplain. This finding is consistent with our own monitoring of floodplain sedimentation upstream on the lower Cosumnes River floodplain and the extensive literature that has demonstrated a strong correlation between distance from the channel and event-based (e.g., Asselman and Middelkoop, 1995; Steiger *et al*., 2001) or decadal-scale (e.g., Kleiss, 1996; Allison *et al*., 1998; Goodbred and Kuehl, 1998; Walling and He, 1998; Walling *et al*., 1998) sedimentation rates. It is also consistent with the demonstrated relationship between the deposition of sand and channel proximity during flood events (e.g., Jacobson and Oberg, 1997; Ten Brinke *et al*., 1998; Florsheim and Mount, 2002). In consequence, we interpret the units dominated by fine sediment as overbank flood deposits that were laid down more slowly and distal to the channels. Thick coarse

sand units may be either channel deposits or near-channel overbank flood deposits (Walling *et al*., 1997; Walling and He, 1998; Tornqvist and Bridge, 2002). Our monitoring of sediment deposition on the floodplain in the lower Cosumnes has also found that gravel is only deposited in-channel and not on the floodplain surface.

Tract elevation

The age–depth model (Figure 3) suggests that the surface of MWT may have been highly variable in the past. For example, at 6500 cal BP the model indicates an ~7 m difference in elevation between MWT-6 and MWT-8, which are only 1 km apart (Figures 1 and 3). Yet, it is hypothesized that the overall surface of the MWT upper deltaic plain was likely subdued through time with only a small elevation gradient in a downstream direction. Perhaps elevational gradients between different depositional facies on MWT such as natural levees or channels could account for the apparent differences in the age–depth model. Indeed, Tornqvist and Bridge (2002) show a rapid decrease of several meters in overbank sediment deposition away from the channel. Alternatively, this pattern could be an artifact of an age–depth model limited by few dates.

Historical maps of the Sacramento River floodplain 22 km upstream of MWT show natural channel levees that are 5 m high adjacent to the channel and 1·5 m high 1 km away (Atwater *et al*., 1979), yielding a 3·5 m range over the same distance as that between the MWT coring sites, suggesting that a natural levee could possibly account for some but not all of the elevation difference between cores. Natural levees along Snodgrass Slough in a protected state park opposite MWT show that in this region of the upper deltaic plain levees rise only 25–30 cm above the interior plain surface over a 20 m lateral extent (Atwater, 1980), further indicating that natural levee deposits, if indeed present in the cores, can only account for some of the observed differences.

Another mechanism that could account for the observed elevation pattern between cores is related to channel depth. The present-day Sacramento River has a typical channel depth of ~8–11 m, whereas the Mokelumne River adjacent to the eastern side of MWT (Figure 1) has a channel depth of 3–4·5 m. Around 6500 cal BP, MWT-6 was characterized by fine sediment and was at the highest elevation (Figures 4 and 7), whereas MWT-2 was intermediate in elevation and aggrading sand. MWT-8 was lowest in elevation and aggrading sand and fine gravel. These observations suggest that the lowest elevation at MWT-8 existed because there was a sand and fine-gravel bedded channel there at 6500 cal BP, and that a smaller channel or inset bar was present at the MWT-2 site. The gravel in MWT-8 is concurrent with the start of increased sedimentation rates in MWT-8 (Figure 5). However, the lack of bracketing radiocarbon dates coupled with the coarse sampling resolution makes it impossible to determine the exact sedimentation rate of this deposit, though it is thought to have been rapid. In contrast, MWT-6 was apparently located more distal to the paleochannels at this time, as evidenced by the presence of silt and clay. It is envisioned that the channels incised into the floodplain, removed underlying fines, and subsequently were followed by channel accretion. These data suggest that MWT was dissected by anastomosing or distributary secondary channels in the past. Thus, the observed 7 m elevational difference between cores could indeed be explained by channel processes and later abandonment.

A third possible explanation for the apparent elevational difference between cores is related to radiometric dating of organic material preserved in fluvial sediments. The observed endmember mixing relationship between particulate organic matter and grain size on MWT (Figure 9) suggests that organic matter is eroded, transported, and deposited concomitant with fine mineral sediment during overbank floods. Asselman and Middelkoop (1995) and Walling *et al*. (1997) note a similar relationship where maximum organic matter coincides to sediment dominated by clay. The near-zero fines intercept in Figure 9 suggest that flooding is the primary mechanism responsible for particulate organic matter deposition on the floodplain and that little of the *in situ* organic matter from floodplain vegetation is preserved unless in a reducing wetland environment, which was observed only in MWT-8. Thus, while organic matter plays only a small role in local accretion on the upper delta plain, it can be derived from reworked upstream floodplain sources. It is, therefore, conceivable that some of the radiocarbon ages are not contemporaneous with sediment deposition due to carbon storage and reworking. For example, recycling of carbon could account for the presence of the somewhat older sediment near the surface in MWT-6 (Table II; Figure 4). The presence of a highly suspicious radiocarbon date of $20\,160 \pm 170$ ^{14}C ybp at 420–430 cm depth in MWT-2 certainly suggests that older carbon has been periodically reworked through the system. Not surprising, these apparently older ages are contained in mineral-dominated sediment that certainly could contain older reworked carbon.

Environmental history

Zone MWT2-1 is highly anomalous because it is considerably older than any other core zone. It is also characterized by fine sediment with high magnetic susceptibility (Table II; Figures 4 and 9) that is atypical relative to other zones that show fines are typically characterized by low magnetic susceptibility. The origins and reasons for the elevated magnetic susceptibility measurements in the fine sediments found in MWT2-1 are currently not known. The chronology for MWT-2 suggests that these sediments were laid down during the mid-Wisconsin interstadial. Verosub *et al*. (2001) show that glacial-aged sediment has a higher magnetic susceptibility than interglacial sediment that is often diluted by soil forming (organic) processes. Perhaps zone MWT2-1 has a high magnetic susceptibility because the overall amount of inorganic sediment that was transported during the cool mid-Wisconsin interstadial was greater than the warmer Holocene (Adam and West, 1983). The high percentage of fines coupled with LOI values that are consistent with the established floodplain mixing line (Figure 8) suggest that floodplains were prevalent in the location of MWT during the mid-Wisconsin. The pollen from MWT2-1 implies the landscape was likely open and consisted of widespread savanna with riparian vegetation and wetlands occurring along riverbanks.

The interval from $23\,550 \pm 210$ to $12\,420 \pm 90$ ^{14}C ybp identified in MWT-2 spans the late-Wisconsin glaciation (Bischoff and Cummins, 2001). This interval is characterized by either extremely slow sedimentation rates or by a glacial hiatus such as a paraconformity. At this time, lowered sea level would have promoted fluvial incision and little or no sediment is expected to have accumulated at the location of MWT because it would have bypassed the site due to the lack of a proximal base-level control.

The post-glacial interval, however, is well represented on MWT with all three cores spanning most or all of the Holocene. The variety of core characteristics reveal that several depositional facies occurred on MWT throughout the Holocene, implying that it was a highly dynamic and variable site that supported a mosaic of habitats. The relationship of grain size and sedimentation rates to channel proximity suggests that the coarse units in MWT6-1 and MWT8-2 (Figures 4 and 9) are either channel or near-channel overbank deposits because of the higher sedimentation rates (Figure 5) compared to other coarse units up-core. The coarse units in MWT2-3 (Figure 4) also likely reflect channel or near-channel deposits, though the origins of these deposits are less certain given that the relationship between sedimentation rates and coarse sediment input is less understood for MWT-2 compared to MWT-6 and MWT-8 (Figure 6). Thus, sedimentation and grain-size data from the cores imply that several episodes of post-glacial channel incision occurred on MWT. Riparian ecosystems and floodplain habitat would have flanked these channels as they drifted across the tract.

Down-core grain-size profiles (Figure 7) provide insight into the long-term history and dynamics of MWT and reveal that two dominate hydrological features operated on the tract in past, namely fine-coarse sediment cycles or fluctuations superimposed on general upward fining. The fine–coarse sediment fluctuations are evident in all cores, though they are not as prominent in MWT-8 compared to cores 2 and 6. The fine–coarse fluctuations in MWT-2 show that the fine sediment content during low-energy periods changed from 50 to 75 to 95 per cent at about 7000, 3500, and 500 cal BP respectively, whereas the fine sediment content during high-energy periods changed from 20 per cent at 6000 cal BP depth to 60 per cent at 1000 cal BP. In MWT-6, the low-energy periods have 75, 90, and 95 per cent fine content at 8000, 6000, and 3000 cal BP, while the high-energy periods have 20 per cent and 40 per cent fines at 7000 and 5000 cal BP respectively. The fine–coarse fluctuations are less evident in MWT-8 because most of MWT-8 spans only the mid- to late-Holocene and it was likely located more distal to the active channel in a quiescent area that experienced organic sediment accumulation during the late-Holocene. We propose that the fluctuations in grain size mainly reflect changes in depositional settings from in-channel to near-channel and distal-channel, though overbank flooding must also be considered since floods of different intensity can not only affect the type of sediment being deposited but also the distance from the channel in which it is eventually laid down. Large flood events are capable of depositing coarse sediment further from the channel compared to smaller floods and such pulsed events could be mistaken for facies changes. Evidence that floods of different intensity occurred on MWT in the past is found in several of the coarse-grained units where interbedded sand, silt, and clay are observed (Figure 4).

As noted previously, coarse sediment is laid down in the channel. On the floodplain, coarse sediment is deposited proximal to the channel during overbank flooding whereas fine sediment is deposited more distal to

the channel. Indeed, ongoing monitoring of sediment deposition on the lowermost floodplain of the Cosumnes River 4 km upstream of MWT show that coarse sand similar to what is observed in the cores is carried onto the floodplain surface on an annual basis (Florsheim and Mount, 2002). The down-core fluctuations in grain size reveal that, through time, channels migrated across MWT and consequently changed the spatio-temporal depositional setting of the tract. A specific example of channel migration and the resulting change in depositional setting can be found in MWT-8 where the switch from largely inorganic sediment deposition to increased organic content at about 5500 cal BP suggests that a slough migrated away from the core site at this time, enabling wetland formation and organic accumulation.

Examination of temporal grain-size fluctuations suggests that the earliest episode of channel incision and lateral migration occurred in the bottom of MWT2-3. This channel is contemporaneous with the late-glacial interval in the Sierra Nevada between roughly 13 000 and 10 000 cal BP. The late-glacial climate history of California is complex and variable. Perhaps these sediments reflect (fluvial) remobilization of widespread glacial sediment (Bursik and Gillespie, 1993; Clark and Gillespie, 1997; James *et al*., 2002) from late-Pleistocene glacial melt-water discharge or in response to a relatively cool wet, and possibly stormy, late-Pleistocene climate as suggested by geomorphic evidence and pollen transfer functions (Adam and West, 1983; Rypins *et al*., 1989; Reneau *et al*., 1990). The next episode of channel incision is noted in MWT6-1. A channel migrated in the MWT-6 location before 9500 cal BP and this channel may have persisted there throughout much of the early-Holocene. Channel deposits are also noted in the mid-Holocene. For example, coarse sediment is observed in the top of MWT2-3 and in MWT8-2 between 7000 and 4000 and between 6600 and 5400 cal BP respectively, suggesting that channels were cross-cutting MWT at this time as well.

The present-day Mokelumne River bounds the MWT to the east (Figure 1). It is conceivable that the ancestral Mokelumne River flowed over MWT at various times in the past and that the coarse sediments noted in the cores are lateral migration lag deposits left behind and covered by fine floodplain sediment. The presence of gravel and other coarse sediment in the cores reveals that the channel was characterized by a relatively high-energy flow regime. We favour the Mokelumne River over the larger and nearby Sacramento River (presently located within 1 km to the west of MWT) as a possible source for these coarse deposits noted in the cores because they are quite thin and we reason that channel gravel and sand deposits from a large river like the Sacramento would have been relatively thick. Another explanation, however, is that numerous small distributary or anastomosing channels diachronously cross-cut MWT in the past.

The general upward-fining trend evidenced in the down-core grain-size profiles (Figure 7), on the other hand, may be attributed to a combination of two possible mechanisms, namely self-limiting overbank deposition as floodplain elevation increased (Wolman and Leopold, 1957) or decreasing competence as sea-level rise reduced flood-pulse energy slopes. Following each flood event on MWT, sediment accumulation elevated the floodplain surface and thus reduced the energetics and duration of future potential overbank deposition. Lithological evidence from the cores such as interbedded clay, silt, and sand indicates that flooding was an important process that accreted the floodplain surface and thus contributed to the upward fining trend. In additional, several researchers (Atwater *et al*., 1979; Atwater and Belknap, 1980; Goman and Wells, 2000) have noted that rapid marine transgression averaging about 2 cm per year occurred in the San Francisco Bay and western Sacramento–San Joaquin Delta between roughly 11 400 and 7000 cal BP. This phase of transgression flooded low-lying coastal communities and moved the shorelines inland by as much as 30 m per year (Atwater, 1979). Transgression slowed to about 0·1–0·2 cm per year at about 7000 cal BP, after which salt marshes managed to keep abreast to the slowly rising sea levels. Continued transgression throughout the Holocene suggests that rising sea levels did indeed decrease flood-pulse energy slopes through time. Thus, it appears that both flooding and flood-pulse energy slopes were both important factors contributing to long-term upward fining trend noted in the cores.

The presence of peat and organic clay deposits containing Cyperaceae pollen in MWT-8 at 5–8 m depth shows unequivocally that freshwater wetlands developed and persisted in the northwest corner of MWT during the mid-Holocene from 5500–4000 cal BP. At this time, sea level was also about 5–7 m lower than present (Atwater, 1979), suggesting that mid-Holocene wetlands may have been under tidal influence and diurnally saturated. Examination of MWT core elevations through time and relative to Holocene sea level (Figure 10) shed insight into when MWT first came under tidal influence. Channels adjacent to MWT presently experience a tidal range of ~1–1·4 m, so any time that past sea level is within ~70 cm of past MWT elevations a tidal influence could

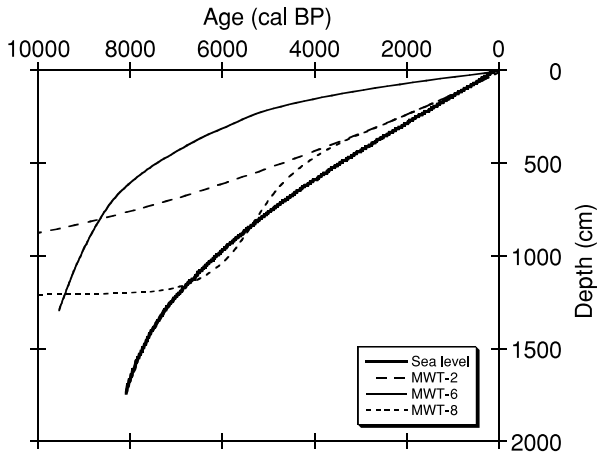

Figure 10. Elevation comparison between a sea-level curve from San Francisco Bay (Atwater, 1979) and the cores from MWT. Channels juxtaposed to present-day MWT have a 1–1·4 m tidal range. Therefore, core depths that are 0·5–0·7 m or more above mean sea level represent intervals when the tract was not under tidal influence, whereas those below this level experienced tidal influence

be present. Before 8000 cal BP there is strong deviation between sea level and core elevation, with sea level being a minimum of about 5 m below the cores, implying that MWT was not under tidal influence at that time. Channel incision occurred at MWT-8 between 7000 and 5500 cal BP and lowered the elevation of MWT-8 to slightly below that of sea level. By 5500 cal BP the elevation of the wetlands in MWT-8, which is constrained by two very reliable AMS dates, is below that of sea level, suggesting that MWT may have come under tidal influence sometime between 8000 and 5500 cal BP, likely at about 6500 cal BP (Figure 10). This interval is certainly contemporaneous to when sea level transgression slowed and wetlands started to keep pace with sea level rise (Atwater, 1979) – tantalizing observations that suggest MWT may indeed have been under tidal influence in the early mid-Holocene. However, an alternate, and more likely, explanation for MWT-8 is that meander cut-off or channel avulsion (Tornqvist and Bridge, 2002), as evidenced by the profound change in grain size over a relatively short time interval, resulted in oxbow formation with subsequent organic accumulation. In this scenario, MWT-8 may have been below sea level, but not under tidal influence. At 8000 cal BP both MWT-2 and MWT-6 consisted of fine floodplain sediment and were above sea level. Channels incised both sites at 7000 and 8000 cal BP respectively, though the amount of incision did not lower the sites below sea level. In fact, by 6000 cal BP deposition of fines was recurring at MWT-6, implying that the channel had migrated away from the site and it was slowly accreting. In contrast, the channel persisted at or near MWT-2 until about 4000 cal BP, at which time the elevation of the site was similar to that of MWT-8 and nearing that of sea level. By about 2500 cal BP, both MWT-2 and MWT-8 were within the 70 cm sea-level differential range. Thus, it seems reasonable to infer that large sections of MWT came under tidal influence at that time. MWT-6, on the other hand, remained above sea level until very recently. These observations confirm that rising tides must have contributed to the long-term fining upward trend observed in the cores, especially during the late-Holocene.

One interesting aspect of the wetland strata is that they contain the most charcoal observed in any of the cores. The general lack of charcoal in the MWT cores suggests that the site did not burn in the past and that flooding was the primary disturbance mechanism. The lack of fire on MWT is likely related to the moist conditions that prevailed in both the riparian zone and the floodplain, though fuel discontinuity was also a factor on the floodplain. The lack of *in situ* charcoal horizons in the peat coupled with frequent saturation due to tidal influence reveals that the wetlands did not burn. Instead, the increase in charcoal in MWT8-3 is hypothesized to be related to the interception of charcoal by dense wetland vegetation (Brown and Hebda, 2002b) as it was transported downstream. In this case, the charcoal is likely from upland sites that were perhaps deliberately burned by native people to increase sustenance yield.

After 4000 cal BP, fines with organics are ubiquitous over MWT (Table II; Figure 4). The generally high concentration of fines on MWT after 4000 cal BP and the lack of coarse deposits suggests that the tract has not

recently been cross-cut by major sand-bearing channels and that the present-day configuration of major channels was established about 4000 years ago. Adam and West (1983) and more recently Anderson (1990) show that late-Holocene climate in California was characterized by increasing precipitation and decreasing temperatures, ushering in a Neoglacial period in the Sierra Nevada (Clark and Gillespie, 1997). The increase in precipitation partially offset the affects of self-limiting overbank deposition and decreased flood-pulse energy slopes. During the last 4000 years, flooding on MWT led to at least 4·5 m of fine accumulation at MWT-2 and MWT-8 and about 1·5 m at MWT-6. Because MWT-6 is much higher in elevation compared to MWT-2 and MWT-8 during this period (Figure 10), it received less overall sediment, which could account for the thinner deposit at that site. The mottles noted in the tops of all cores (Figure 4) are consistent with our interpretation of the late-Holocene since they imply sediment mixing consistent with tidal activity and periodic flooding.

Historic maps show that the entire surface of MWT supported freshwater wetland habitat by 1903 AD (United States Geological Survey, 1911). These wetland deposits are no longer present in the tops of cores due to oxidation and plowing into the agricultural horizon, as evidenced by crop pollen. However, Delta Meadows State Park west of MWT along Snodgrass Slough still has such freshwater wetlands, and they are tidally inundated. Thus, sometime within the last few millennia the entire fine sediment surface of MWT came under direct tidal action yielding a tidal freshwater wetland. The core sediments show that even though the modern wetland had a higher organic content, delta accretion was still inorganic sediment dominated. Thus, vegetation in this region is opportunistically occurring on the surface and not significantly contributing to delta evolution.

In summary, it is possible to extract the unique elements of an upper deltaic plain that distinguish it from a floodplain and the rest of the delta based on the results of this study. In this case, the delta is forming over a floodplain as sea level rises, whereas in other situations open-water receiving basins form deltas that eventually aggrade into floodplains. Similar to floodplains, an upper deltaic plain has cyclic coarse–fine geomorphic units created by alternating lateral migration and overbank deposition. However, unlike a floodplain, the surface of an upper deltaic plain consists of poorly drained silt and clay forming a permanent wetland with a very thin veneer of vegetation and organic matter. By contrast, lower deltaic zones have a significantly higher proportion of vertical accretion due to peat formation, as evidenced on other tracts downstream of MWT in the Sacramento–San Joaquin Delta (Atwater, 1980).

CONCLUSION

The multi-proxy records from MWT provide insight into the dynamics of an upper deltaic plain in the Sacramento–San Joaquin Delta, California. These records show that (1) coarse-grained sediment accretes vertically more rapidly, has greater sedimentation rates, and higher magnetic susceptibility values compared to fine-grained sediment and this pattern is related to proximity to channel and flood regime; (2) particulate organic matter that washes off hillslopes during winter storms and spring snowmelt is deposited on the floodplain with fine inorganic sediment during overbank flooding; (3) the persistent fraction of organic matter that survives transport, deposition, and possible diagenesis is 5·5 per cent of the total sediment mass; (4) two hydrological domains are evident in the MWT cores, coarse–fine fluctuations superimposed on general upward fining; (5) the fine–coarse grain size fluctuations are reflective of spatio-temporal changes in depositional settings as well as variations in flood intensity; (6) the upward fining trend is related to self-limiting overbank deposition and reduced flood-pulse energy slopes associated with post-glacial marine regression; (7) throughout its history, the MWT (and by inference other tracts in the delta) were cross-cut by numerous channels and subjected to frequent flooding; (8) MWT first came under tidal influence at about 2500 cal BP; (9) floodplain sediment containing >90 per cent fines should be targeted for pollen extraction; and (10) fire is not a common type of disturbance on the upper deltaic plain though wetland interception of charcoal can lead to charcoal accumulation. In summary, our findings reveal that upper delta plains do indeed have a distant geomorphology from floodplains and lower deltaic regions.

ACKNOWLEDGEMENTS

The authors kindly thank the Seaver Institute, University of California, and CALFED (Ecosystem Restoration Program Co-op Agreement no. 114200J095) for providing funding for this research. Jeff Mount and Ken

Verosub were especially helpful, providing thoughtful comments and insight into the delta region. In addition, J. Mount kindly contributed considerable financial resources for analytical equipment used in this investigation and K. Verosub graciously permitted access to his magnetics laboratory and use of his equipment. We would also like to thank Drs Roger Byrne, Robert Zierenberg, Mike Singer, Gary Weissmann, Ramona Swenson, and Jim Clark for their thoughts and comments. We thank the Nature Conservancy for access to their land, help in field logistics, and partnership in research, outreach, and education. We are grateful to Ellen Mantalica, Kaylene Keller, Derek Sappington, Mike Bezemek, Laurel Aroner, Wendy Trowbridge, Jim MacIntyre, Jose Constantine, and the numerous other volunteers for their assistance. Finally, we sincerely thank two anonymous reviewers who provided thorough and constructive comments that improved the manuscript.

REFERENCES

Adam DP, West GJ. 1983. Temperature and precipitation estimates through the last glacial cycle from Clear Lake, California, pollen data. *Science* **219**: 168–170.

Alexander J, Marriott S. 1999. Introduction. In *Floodplains: Interdisciplinary Approaches*, Alexander J, Marriott S (eds). Special Publication 163. Geological Society of London; 1–13.

Allison MA, Kuehl SA, Martin TC, Hassan, A. 1998. Importance of flood-plain sedimentation for river sediment budgets and terrigenous input to the oceans: insights from the Brahmaputra Jamuna River. *Geology* **26**: 175–178.

Anderson RS. 1990. Holocene forest development and paleoclimates within the central Sierra Nevada, California. *Journal of Ecology* **78**: 470–489.

Asselman NEM, Middelkoop H. 1995. Floodplain sedimentation: quantities, patterns and processes. *Earth Surface Processes and Landforms* **20**: 481–499.

Atwater BF. 1979. Ancient processes at the site of Southern San Francisco Bay, movement of the crust and changes in sea level. In *San Francisco Bay: The Urbanized Estuary*, Conomos TJ (ed). American Association for the Advancement of Science, Pacific Division: San Francisco; 31–45.

Atwater BF. 1980. Distribution of vascular-plant species in six remnants of intertidal wetland of the Sacramento–San Joaquin Delta, California. *US Geological Survey Open-File Report 80–833*: 1–45.

Atwater BF, Belknap DF. 1980. Tidal-wetland deposits of the Sacramento–San Joaquin Delta, California. In *Quaternary Depositional Environments of the Pacific Coast, Pacific Coast Paleogeography Symposium 4*, Field ME, Douglas RG, Bouma AH, Ingle JC, Colburn IP (eds). Pacific Section of the Society of Economic Paleontologists and Mineralogists: Los Angeles; 89–103.

Atwater BF, Conard SG, Dowden JN, Hedel CW, MacDonald RL, Savage W. 1979. History, landforms, and vegetation of the estuary's tidal marshes. In *San Francisco Bay: The Urbanized Estuary*. Conomos TJ (ed.). American Association for the Advancement of Science, Pacific Division: San Francisco; 347–385.

Band JW. 1998. Neotectonics of the Sacramento–San Joaquin Delta Area, East-Central Coast Ranges, California. PhD dissertation: University of California, Berkeley.

Benda L, Dunne T. 1997. Stochastic forcing of sediment routing and storage in channel networks. *Water Resources Research* **33**: 2865–2880.

Berry LG, Mason B. 1983. *Mineralogy* (2nd edn). W. H. Freeman: New York.

Beuning KRM, Talbot MR, Kelts K. 1997. A revized 30 000-year paleoclimatic and paleohydrologic history of Lake Albert, east Africa. *Palaeogeography, Palaeoclimatology, and Palaeoecology* **136**: 259–279.

Bischoff JL, Cummins K. 2001. Wisconsin glaciation of the Sierra Nevada (79 000–15 000 yr B.P.) as recorded by rock flour in sediments of Owens Lake, California. *Quaternary Research* **55**: 14–24.

Black CA. 1965. *Methods of Soil Analysis, Part 1*. American Society of Agronomy: Madison, WI.

Blum MD, Tornqvist TE. 2000. Fluvial responses to climate and sea-level change: a review and look forward. *Sedimentology* **47**: 2–48.

Brakenridge GR. 1980. Widespread episodes of stream erosion during the Holocene and their climatic cause. *Nature* **283**: 655–656.

Bridge JS. 1984. Large-scale facies sequences in alluvial overbank environments. *Journal of Sedimentary Petrology* **54**: 583–588.

Brooks J, Elsik WC. 1974. Chemical oxidation (using ozone) of the spore wall of *Lycopodium clavatum*. *Grana* **14**: 85–91.

Brown AG. 1997. *Alluvial Geoarchaeology: Floodplain Archaeology and Environmental Change*. Cambridge University Press: Cambridge, CA.

Brown KJ, Hebda RJ. 2002a. Origin, development, and dynamics of coastal temperate conifer rainforests of southern Vancouver Island, Canada. *Canadian Journal of Forest Research* **32**: 353–372.

Brown KJ, Hebda RJ. 2002b. Ancient fires on southern Vancouver Island, British Columbia, Canada: a change in causal mechanisms at about 2,000 years BP. *Environmental Archaeology* **7**: 1–13.

Bursik MI, Gillespie AR. 1993. Late Pleistocene glaciation of Mono Basin, California. *Quaternary Research* **39**: 24–35.

Campbell ID. 1991. Experimental mechanical destruction of pollen grains. *Palynology* **15**: 29–33.

Catto NR. 1985. Hydrodynamic distribution of palynomorphs in a fluvial succession, Yukon. *Canadian Journal of Earth Science* **22**: 1552–1557.

Clark DH, Gillespie AR. 1997. Timing and significance of Late-Glacial and Holocene cirque glaciation in the Sierra Nevada, California. *Quarternary International* **38/39**: 21–38.

Coleman JM. 1976. *Deltas: Processes of Deposition and Models for Exploration*. Continuing Education Publication Company: Champagne, IL.

Conomos TJ, Peterson DH. 1976. Suspended-particle transport and circulation in San Francisco Bay: an overview. In *Estuarine Processes*. Vol. 2: *Circulation, Sediments, and Transfer of Materials in the Estuary*, Wiley M (ed.). Academic Press: New York; 82–97.

Constantine JC, Pasternack GB, Johnson MB. 2003. Floodplain evolution in a small, tectonically active basin of northern California. *Earth Surface Processes and Landforms* **28**: 869–888.

Cotton JA, Heritage GL, Large ARG, Passmore DG. 1999. Biotic response to late Holocene floodplain evolution in the River Irthing catchment, Cumbria. In *Floodplains: Interdisciplinary Approaches*, Marriot SB, Alexander J (eds). Special Publication 163. Geological Society, London; 163–178.

Fall PL. 1987. Pollen taphonomy in a canyon stream. *Quaternary Research* **28**: 393–406.

Fisk HN. 1944. Geological investigation of the alluvial valley of the lower Mississippi River. Mississippi River Commission: Vicksburg.

Florsheim JL, Mount JF. 2002. Restoration of floodplain topography by sand–splay complex formation in response to intentional levee breaches, Lower Cosumnes River, California. *Geomorphology* **44**: 67–94.

Florsheim JL, Mount JF. 2003. Changes in lowland floodplain sedimentation processes: pre-disturbance to post-rehabilitation, Cosumnes River, California. *Geomorphology* **56**: 305–323.

Folk RL. 1974. *Petrology of Sedimentary Rocks*. Hemphill: Austin, TX.

Galloway WE. 1975. Process framework for describing the morphologic and stratigraphic evolution of deltaic depositional systems. In *Deltas: Models for Exploration*, Broussar ML (ed.). Houston Geological Society: Houston, TX; 87–98.

Goman M, Wells L. 2000. Trends in river flow affecting the northeastern reach of the San Francisco Bay estuary over the past 7000 years. *Quaternary Research* **54**: 206–217.

Goodbred SL, Kuehl SA. 1998. Floodplain processes in the Bengal Basin and the storage of Ganges–Brahmaputra river sediment: an accretion study using ^{137}Cs and ^{210}Pb geochronology. *Sedimentary Geology* **121**: 239–258.

Havinga AJ. 1967. Palynology and pollen preservation. *Review of Palaeobotany and Palynology* **2**: 81–98.

Hickman J (ed.). 1996. *The Jepson Manual, Higher Plants of California*. University of California Press: Berkeley, CA.

Holloway RG. 1989. Experimental mechanical pollen degradation and its applications to Quaternary age deposits. *Texas Journal of Science* **41**: 131–145.

Hudson-Edwards KA, Macklin MG, Taylor MP. 1999. 2000 years of sediment-borne heavy metal storage in the Yorkshire Ouse basin, NE England, UK. *Hydrological Processes* **13**: 1087–1102.

Jacobson RB, Oberg KA. 1997. Geomorphic changes on the Mississippi River floodplain at Miller City, Illinois, as a result of the flood of 1993. *US Geological Survey Circular 1120-J*: 1–22.

James LA, Harbour J, Fabel D, Dahms D, Elmore D. 2002. Late Pleistocene glaciations in the northwestern Sierra Nevada, California. *Quaternary Research* **57**: 409–419.

Jervey MT. 1988. Quantitative geological modeling of siliciclastic rock sequences and their seismic expression. In *Sea-Level Changes: An Integrated Approach*, Wilgus CK, Hastings BS, Kendall CGSC, Posamentier HW, Ross CA, Van Wagoner JC (eds). Special Publication 42. Society of Economic Paleontologists and Mineralogists: Tulsa; 47–69.

Kleiss BA. 1996. Sediment retention in a bottomland hardwood wetland in eastern Arkansas. *Wetlands* **16**: 321–333.

Knight MA, Pasternack GB. 2000. Sources, input pathways, and distributions of Fe, Cu, and Zn in a Chesapeake Bay tidal freshwater marsh. *Environmental Geology* **39**: 1359–1371.

Knox JC. 1993. Large increases in flood magnitude in response to modest changes in climate. *Nature* **361**: 430–432.

Knox JC. 1995. Fluvial systems since 20 000 yrs B.P. In *Global Continental Palaeohydrology*, Gregory KJ, Starkel L, Baker VR (eds). Wiley: Chichester; 87–108.

Logan SH. 1990. Global warming and the Sacramento–San Joaquin Delta. *California Agriculture* **44**: 16–18.

Mattraw HC, Elder JF. 1984. *Nutrient and detritus transport in the Apalachicola River, Florida*. Water-Supply Paper 2196-C. US Geological Survey, Washington, DC.

Moore PD, Webb JA, Collinson ME. 1991. *Pollen Analysis* (2nd edn). Blackwell Scientific: Oxford.

Nanson GC. 1986. Episodes of vertical accretion and catastrophic stripping: a model of disequilibrium flood-plain development. *Geological Society of America Bulletin* **97**: 1467–1475.

Noble RA, Wu CH, Atkinson CD. 1991. Petroleum generation and migration from Talang Akar coals and shales offshore NW Java, Indonesia. *Organic Geochemistry* **17**: 363–374.

Orton GJ, Reading HG. 1993. Variability of deltaic processes in terms of sediment supply, with particular emphasis on grain size. *Sedimentology* **40**: 475–512.

Pasternack GB, Brush GS. 2001. Seasonal variations in sedimentation and organic content in five plant associations on a Chesapeake Bay tidal freshwater delta. *Estuarine, Coastal, and Shelf Science* **53**: 93–106.

Pasternack GB, Brush GS. 2002. Biogeomorphic controls on sedimentation and substrate on a vegetated tidal freshwater delta in upper Chesapeake Bay. *Geomorphology* **43**: 293–311.

Pasternack GB, Brush GS, Hilgartner WB. 2001. Impact of historic land-use change on sediment delivery to an estuarine delta. *Earth Surface Processes and Landforms* **26**: 409–427.

Rainwater EH. 1975. Petroleum in deltaic sediments. In *Deltas: Models for Exploration*, Broussard ML (ed.). Houston Geological Society: Houston, TX; 3–11.

Reneau SL, Dietrich WE, Donahue DJ, Jull AJT, Rubin M. 1990. Late Quaternary history of colluvial deposition and erosion in hollows, central California Coast Ranges. *Geological Society of America Bulletin* **102**: 969–982.

Rojstaczer SA, Hamon RE, Deverel SJ, Massey CA. 1991. Evaluation of selected data to assess the causes of subsidence in the Sacramento–San Joaquin Delta, California. *US Geological Survey Open-File Report* **91–193**: 1–16.

Rypins S, Reneau SL, Byrne R, Montgomery DR. 1989. Palynologic and geomorphic evidence for environmental change during the Pleistocene–Holocene transition at Point Reyes Peninsula, Central Coastal California. *Quaternary Research* **32**: 72–87.

Sander PM, Gee CT. 1990. Fossil charcoal: techniques and applications. *Review of Palaeobotany and Palynology* **63**: 269–279.

Singer MJ, Verosub KL, Fine P, TenPas J. 1996. A conceptual model for the enhancement of magnetic susceptibility in soils. *Quaternary International* **34–36**: 243–248.

Steiger J, Gurnell AM, Petts GE. 2001. Sediment deposition along the channel margins of a reach of the middle River Severn, UK. *Regulated Rivers Research and Management* **17**: 443–460.

Stuiver M, Reimer PJ. 1993. Extended ^{14}C database and revised CALIB 3·0 ^{14}C age calibration program. *Radiocarbon* **35**: 215–230.

Ten Brinke WBM, Schoor MM, Sorber AM, Berendsen HJA. 1998. Overbank sand deposition in relation to transport volumes during large-magnitude floods in the Dutch sand-bed Rhine river system. *Earth Surface Processes And Landforms* **23**: 809–824.

Tornqvist TE, Bridge JS. 2002. Spatial variation of overbank aggradation rate and its influence on avulsion frequency. *Sedimentology* **49**: 891–905.
Tu I. 2000. Vegetation patterns and processes of natural regeneration in periodically flooded riparian forests in the Central Valley of California. PhD dissertation, University of California, Davis, CA.
United States Geological Survey. 1911. Topographical map of the Sacramento Valley, California. *US Geological Survey Atlas Sheets.*
Verosub KL, Harris AH, Karlin R. 2001. Ultra-high-resolution paleomagnetic record from ODP Leg 169S, Saanich Inlet, British Columbia: initial results. *Marine Geology* **174**: 79–93.
Walling DE, He Q. 1998. The spatial variability of overbank sedimentation on river floodplains. *Geomorphology* **24**: 209–223.
Walling DE, Owens PN, Leeks GJL. 1997. The characterisitics of overbank deposits associated with a major flood event in the catchment of the River Ouse, Yorkshire, UK. *Catena* **31**: 53–75.
Walling DE, Owens PN, Leeks GJL. 1998. The role of channel and floodplain storage in the suspended sediment budget of the River Ouse, Yorkshire, UK. *Geomorphology* **22**: 225–242.
Wolfe AP, Kaushal SS, Fulton JR, McKnight DM. 2002. Spectrofluorescence of sediment humic substances and historical changes of lacustrine organic matter provenance in response to atmospheric nutrient enrichment. *Environmental Science and Technology* **36**: 3217–3223.
Wolman MG, Leopold LB. 1957. River floodplains: some observations on their formation. Professional Paper 282-C. US Geological Survey.

